Polym. Korea, Vol. 50, No. 1, pp. 14-22 (2026)
https://doi.org/10.7317/pk.2026.50.1.14 ISSN 2234-8077(Online)

반응표면법을 이용한 티타니아가 도입된 PEI–PVAc 복합막의 CO_2/CH_4 분리 효율 최적화

Khuram Maqsood†, Asif Jamil*, Rizwan Nasir, Mustafa Alsaady, and Aymn Bin Abdulrahman
Department of Chemical Engineering, University of Jeddah
*Department of Chemical, Polymer and Composite Materials Engineering, University of Engineering and Technology (New Campus)

(2025년 3월 26일 접수, 2025년 8월 8일 수정, 2025년 9월 15일 채택)

Optimization of CO_2/CH_4 Separation Efficiency of Titania Incorporated PEI-PVAc Composite Membranes through Response Surface Methodology

Khuram Maqsood†, Asif Jamil*, Rizwan Nasir, Mustafa Alsaady, and Aymn Bin Abdulrahman
Department of Chemical Engineering, University of Jeddah, 23890, Saudi Arabia
**Department of Chemical, Polymer and Composite Materials Engineering, University of Engineering and Technology (New Campus), Lahore, 39021, Pakistan*

(Received March 26, 2025; Revised August 8, 2025; Accepted September 15, 2025)

Abstract: This study examines the optimization of CO_2/CH_4 separation utilizing polyetherimide (PEI)-polyvinyl acetate (PVAc) blend membranes augmented by TiO_2 nanoparticles. This study utilizes membrane-based separation procedures, preferred over traditional methods due to their environmental and economic advantages. The gas permeance and selectivity of the membranes were evaluated using a custom gas permeation unit, with variations in temperature, pressure, and nanoparticle composition. A combination of response surface methodology (RSM) and central composite design (CCD) was utilized to forecast and enhance the process elements influencing separation efficiency. The research indicates that TiO_2 nanoparticles markedly improve the separation efficiency of membranes, with the ideal concentration determined to maximize CO_2 permeance while decreasing CH_4 permeance. The experimental results confirmed the predictive accuracy of the created models, evidenced by a R^2 value of 0.9813, indicating a strong fit. The results highlight the promise of nanoparticle-enhanced membranes in industrial applications.

Keywords: response surface methodology, optimization, blend membrane, composite membrane, CO_2 separation.

Introduction

Natural gas is a vital energy resource, contributing approximately 22% to the global energy supply. However, it often contains carbon dioxide (CO_2) as an impurity, which lowers its calorific value and affects overall energy efficiency.[1] The CO_2 in natural gas reacts with water, creating acidic conditions that can damage pipelines and infrastructure.[2] Therefore, removing CO_2 from natural gas is crucial for environmental protection and maintaining its energy value. This has made CO_2 removal a key focus of scientific research, particularly in light of the expected rise in natural gas use and the need to meet pipeline standards.[3,4]

Due to their smaller environmental impact, cleaner production, cost-effectiveness, and energy efficiency, membrane-based separation processes are now preferred over traditional methods like solid adsorption, liquid absorption, and cryogenic distillation.[5] The utilization of membrane technology for CO_2/CH_4 separation has garnered significant attention in various fields, including natural gas sweetening, biogas purification, and water treatment. This technique ensures a high methane recovery rate of over 96% and the ability to capture and reuse pure CO_2.[6] Nevertheless, a notable obstacle with commercial membranes, whether organic or inorganic, is finding the right equilibrium between gas permeability and selectivity.[7]

Polymer blends are a viable approach for producing gas separation membranes. The fundamental problem with this strategy is to ensure compatibility amongst the polymers utilized while preserving essential mechanical qualities.[8] The compatibility can be enhanced by incorporating nanoparticles into polymer blends to enhance their physical and chemical characteristics

---

†To whom correspondence should be addressed.
kmaqsood@uj.edu.sa, ORCID 0000-0003-2049-4274

and promote compatibility. For instance, adding TiO_2 nanoparticles to a polyetherimide (PEI)-polyvinyl acetate (PVAc) blend has been demonstrated to improve the blend's mechanical durability and reduce solvent precipitation, resulting in denser membrane layers and better separation capabilities.[9]

Li *et al*. found that adding TiO_2 nanoparticles to polymer membranes enhanced their mechanical stability.[10] Furthermore, they discovered that adding TiO_2 reduced the rate of solvent precipitation, resulting in a thicker membrane cross-section skin layer. In addition, Madaeni et al. observed improved separation properties and a related increase in the thickness of the membrane wall when TiO_2 nanoparticles were added.[11] Similarly, adding TiO_2 nanoparticles to the PVAc matrix increased the performance and thermal stability of the produced membranes.[12] The gas separation performance of the poly(amide-imide)-TiO_2 nanocomposite membrane surpassed that of pure poly(amide-imide), even with a low TiO_2 loading.[13]

The above-mentioned studies evaluated the incorporation of titania fillers and assessed the physical, mechanical, and separation performance of the membranes. However, the influence of process parameters on membrane performance has not been examined in detail. Notably, operating temperature affects the free volume and flexibility of the polymer matrix, typically enhancing gas permeance while reducing selectivity. Conversely, higher feed pressures can diminish the sorption capacity and gas solubility of the materials, potentially impairing their overall performance.[1,2]

Therefore, in this study, a thorough investigation has been carried out to examine the effect of temperature, total pressure difference, and TiO_2 composition on the permeability of CO_2 and CH_4 and the separation factor between CO_2 and CH_4. The analysis utilized response surface methodology (RSM) and central composite design (CCD) to determine the optimal settings for achieving minimum CH_4 permeance and maximum CO_2 permeance and separation factor.

Experimental

Materials. PEI pellets (melt flow index, 9 g/10 min), PVAc beads (density, 1.19 g/cm^3 at 25 °C), N-methyl-2-pyrrolidone (NMP, 99.5% purity), and TiO_2 nanoparticles (primary particle size 21 nm) were all sourced from Sigma Aldrich (St. Louis, MO, USA).

Membrane Development. By employing a casting knife, the membrane solution was uniformly applied onto a glass plate, forming a film with a thickness of 150 μm. The membranes fabricated in this research included blend polymer and composite membranes, as previously described in our studies.[14,15] The blend membrane consists of a blend ratio of 98:2 for PEI-PVAc. Subsequently, TiO_2 was introduced as a nanofiller into the blend polymer dope solution to develop composite membranes. The titania content was also adjusted from 0 to 2 wt%. The newly formed membranes were chilled in a water bath after casting. The membranes were immersed in distilled water for three days to ensure that all solvent was completely removed. Following that, they were allowed to air dry at room temperature.

Gas Permeation Study of the Developed Membranes: The developed membranes underwent gas permeation and ideal selectivity analysis. For this analysis, CO_2 and CH_4 gases were utilized, with variations in feed pressure and temperature as outlined, Table 1. The data is categorized into input parameters, including permeate temperature, feed pressure, and TiO_2 composition. In contrast, the responsive parameters included the gas permeation rates of CO_2 and CH_4 and the ideal gas selectivity (CO_2/CH_4).

Using a specifically made gas permeation machine for these measurements and determined by the equations, permeability testing for pure gases was carried out on the developed membranes,[15] Equations 1 and 2.

$$P_x/l = \frac{Q}{A\Delta P}\frac{273.15}{T} \tag{1}$$

$$\alpha_{xy} = \frac{P_x}{P_y} \tag{2}$$

Gas permeance (P_x/l) is quantified in GPU, where 'x' in the subscript denotes the incident gas, such as CO_2 or CH_4. Here, 'Q' indicates the volumetric flow rate, and 'A' represents the membrane's effective surface area. The permeation occurs under a specific pressure difference and at a designated temperature (T). The ratio of the competing incident gases' x and y permeabilities through the membrane is ideal selectivity or α_{xy}.

Optimization Strategy by Using RSM: This work used Design of Experiments (DoE) to investigate CO_2 separation and process optimization with PEI-PVAc blend membranes in a methodical manner. A collection of statistical and mathematical methods known as RSM are used to model and analyze situations in which multiple variables affect an interest response. The objective was to maximize that response.

As extensively documented in the literature, the advantages of employing this method include reducing the number of experimental runs, determining optimal operating conditions for scale-up, and understanding the interactions among differ-

Table 1. Experiment Design Matrix and Results for Responses

	Factors			Responses		
No Exp.	Pressure (bar)	Temperature (°C)	TiO_2 Composition (wt%)	CO_2 Permeance (GPU)	CH_4 Permeance (GPU)	Selectivity (CO_2/CH_4)
1	2	25	0	14.86	0.49	30.33
2	4	25	0	14.08	0.5	28.16
3	6	25	0	14.12	0.51	27.69
4	2	25	1	17.31	0.52	33.29
5	4	25	1	17.04	0.51	33.41
6	6	25	1	16.9	0.52	32.50
7	2	25	2	19.72	0.48	41.08
8	4	25	2	19.26	0.51	37.76
9	6	25	2	18.93	0.49	38.63
10	2	35	0	12.01	0.53	22.66
11	4	35	0	11.26	0.56	20.11
12	6	35	0	10.89	0.58	18.78
13	2	35	1	15.02	0.47	31.96
14	4	35	1	14.14	0.48	29.46
15	6	35	1	14.01	0.5	28.02
16	2	35	2	16.31	0.5	32.62
17	4	35	2	15.52	0.51	30.43
18	6	35	2	15.02	0.53	28.34
19	2	45	0	10.42	0.58	17.97
20	4	45	0	10.01	0.57	17.56
21	6	45	0	9.31	0.59	15.78
22	2	45	1	12.98	0.46	28.22
23	4	45	1	12.05	0.47	25.64
24	6	45	1	11.46	0.49	23.39
25	2	45	2	14.28	0.53	26.94
26	4	45	2	13.92	0.56	24.86
27	6	45	2	13.11	0.55	23.84

ent experimental variables.

The dataset encompasses pressure, temperature, and TiO_2 composition, aiming to maximize CO_2 permeance. A quadratic model was applied to the data, integrating both linear and interaction terms of the variables, which aids in elucidating the combined effects of pressure, temperature, and TiO_2 composition on CO_2 permeance.

Similarly, a quadratic model defined the relationship between the variables and selectivity, incorporating linear and interaction effects. This approach provides a comprehensive insight into how each variable impacts the outcome, enhancing understanding of their collective influence on selectivity.

Results and Discussion

The experimental results generated using RSM in combination with CCD are presented along with the corresponding outcomes, Table 2. The CO_2 and CH_4 permeance ranged from 9.31 to 19.72 GPU and 0.46 to 0.59 GPU, respectively. Furthermore, CO_2/CH_4 separation coefficients ranging from 15.78 to 41.08 were attained.

The quadratic model, incorporating coded factors, is recommended by the DoE software for analyzing CO_2 permeance, Equation 3.

Table 2. Ranges of Process Parameters and Their Variations Over the Developed Membranes

Variables	Factor code	Level and range (coded)		
		-1	0	1
Feed pressure (bar)	A	2	4	6
Temperature (°C)	B	25	35	45
TiO_2 composition (wt%)	C	0	1	2

$$Y = \beta_0 + \beta_1 A + \beta_2 B + \beta_3 C + \beta_{12} AB + \beta_{13} AC + \beta_{23} BC + \beta_{11} A^2 + \beta_{22} B^2 + \beta_{33} C^2 \quad (3)$$

CO_2 Permeance. ANOVA outcomes and empirical model factors for CO_2 permeance are highlighted, Table 3. CO_2 selectivity models using both coded and real components are provided, Equation 4.

Based on the data in Table 3, the model's F-value is 437.438, and the associated P-value, less than 0.05, suggests that the model is statistically significant.

$$CO_2 \text{ Permeance} = 27.23 - 0.2049A - 0.6332B + 4.1528C - 0.0078AB - 0.0117AC - 0.0273BC + 0.0292A^2 + 0.0063B^2 - 0.4883C^2 \quad (4)$$

Furthermore, while terms such as A^2 and AC were found to be insignificant, they have been included to maintain the hierarchical structure of the model, Equation 4. Additionally, an R^2 value of 0.996 confirms the model's high accuracy in predicting CO_2 permeance. Regarding the individual effects, the composition of TiO_2 (referred to as term C) had the most notable influence on CO_2 permeance, as indicated by the greatest F-value of 262.91. Temperature (term B) and gas feed pressure (term A) had F-values of 111.349 and 6.693, respectively, suggesting a lesser impact. These results underscore the predominant influence of TiO_2 composition on CO_2 permeance. Meanwhile, the second order (AC and BC) and quadratic terms (A^2, B^2, and C^2) were found to have minimal impact on the CO_2 permeance for blend membranes.

The effect of temperature, feed pressure, and the TiO_2 feed content on the permeance of CO_2 in polymer composite membranes (PCMs) are presented in Figure 1. Figure 1(a) shows a notable decrease in CO_2 permeance as feed pressure increases, consistent with previous studies suggesting a gas permeability reduction for polarizable gases like CO_2 in glassy polymers under elevated pressures.[16] This decline supports the dual-mode sorption hypothesis and is further influenced by membrane matrix contraction, which reduces the membrane's swelling effect, consequently lowering CO_2 permeability.[15,17] Furthermore, as temperature rises, CO_2 diffusivity through the membrane increases, contributing to a minor decrease in CO_2 permeance. However, this decrease is counteracted by reducing adsorption coverage as fewer CO_2 molecules absorb to the membrane surface.[18] The highest recorded CO_2 permeance at 25 ℃ and 2 bar was 17.31 GPU, while the lowest at 45 ℃ and 6 bar was 11.46 GPU.

The effects of temperature and TiO_2 composition on CO_2 permeance at 4 bar are highlighted, Figure 1(b). There is an observed increase in CO_2 permeance with higher TiO_2 composition, with a permeance of 19.26 GPU at 2 wt% TiO_2 and

Table 3. ANOVA Results and Empirical Model Terms of CO_2 Permeance

Sources	Sum of square	DOF	F-Value	PR (>F)	Mean Square	Significance
A	0.345	1	6.693	0.0192	0.349	S[a]
B	5.816	1	111.349	7E-09	5.817	S
C	13.734	1	262.916	8.94E-12	13.734	S
A^2	0.0817	1	1.563	0.228	0.082	N-S[b]
B^2	2.407	1	46.072	3.17E-06	2.407	S
C^2	1.431	1	27.391	6.74E-05	1.431	S
AB	0.288	1	5.519	0.0312	0.288	S
AC	0.007	1	0.125	0.728	0.0065	N-S
BC	0.897	1	17.163	0.0007	0.897	S
Residual	0.888	17	-	-	0.052	N-S
R^2	0.996	-	-	-	-	-
Adjusted R^2	0.993	-	-	-	-	-
Model	205.655	9	437.438	2.61E-18	22.851	S

[a]Significant. [b]Not Significant.

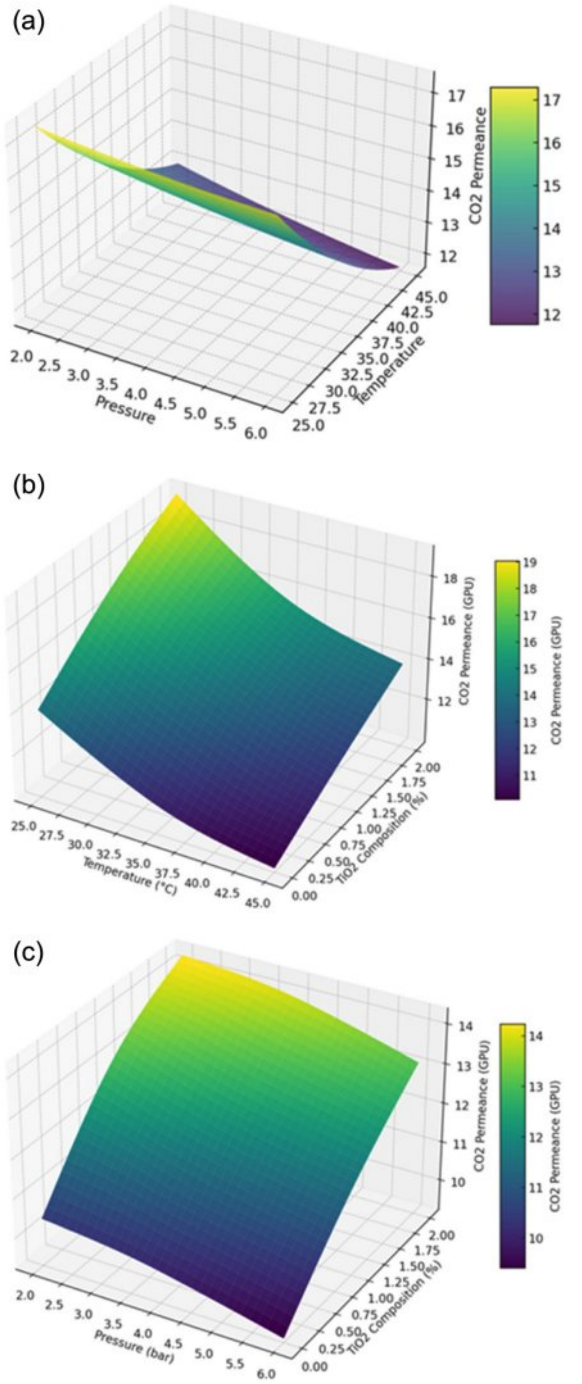

Figure 1. (a) Effect of temperature and pressure on CO_2 permeance at TiO_2 composition of 1 wt%; (b) effect of temperature and TiO_2 composition on CO_2 permeance at 4 bar pressure; (c) effect of pressure and TiO_2 composition on CO_2 permeance at a temperature of 45 °C.

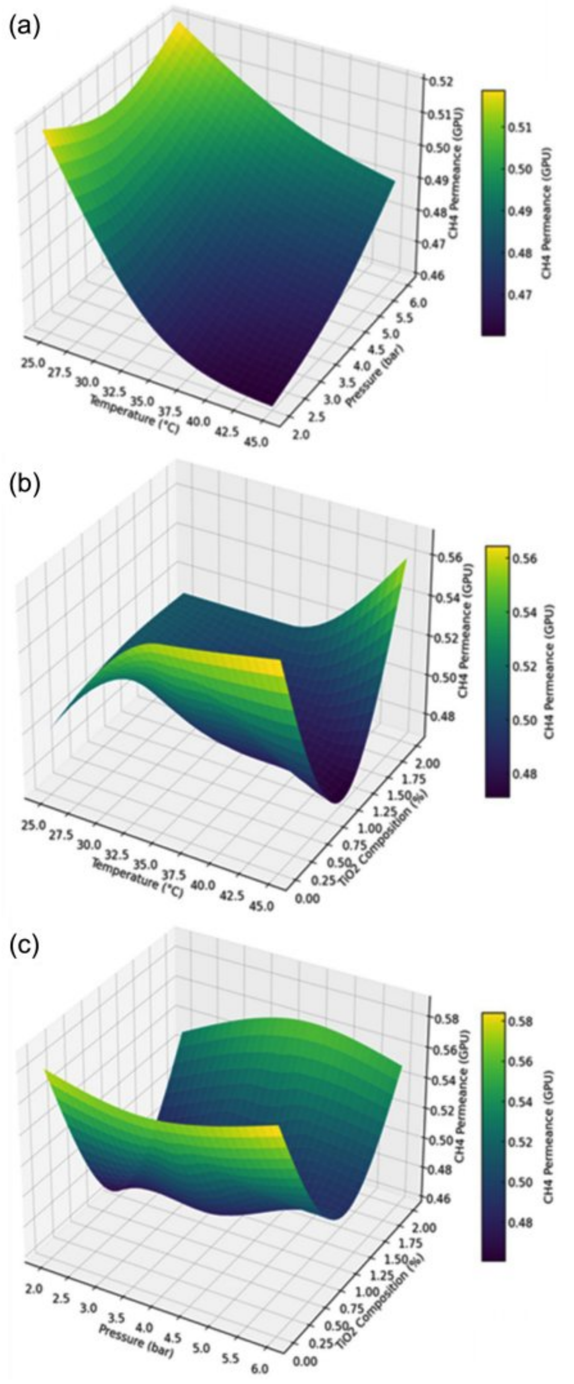

Figure 2. (a) Effect of temperature and pressure on CH_4 permeance at TiO_2 composition of 1 wt%; (b) effect of temperature and TiO_2 composition on CH_4 permeance at 4 bar; (c) effect of pressure and TiO_2 composition on CH_4 permeance at a temperature of 45 °C.

25 ℃. The addition of TiO_2 positively affects the CO_2 permeance, enhancing it by 36% at 2 wt% compared to the neat sample due to nanoparticle aggregation and void formation at the TiO_2-polymer interface, which facilitates gas diffusion.[19] It also indicates that the trend of decreasing CO_2 permeance with rising temperature mirrors the observations, Figure 1(a), with the lowest permeance of 9.31 GPU at 45 ℃ in the absence of TiO_2 nanoparticles.

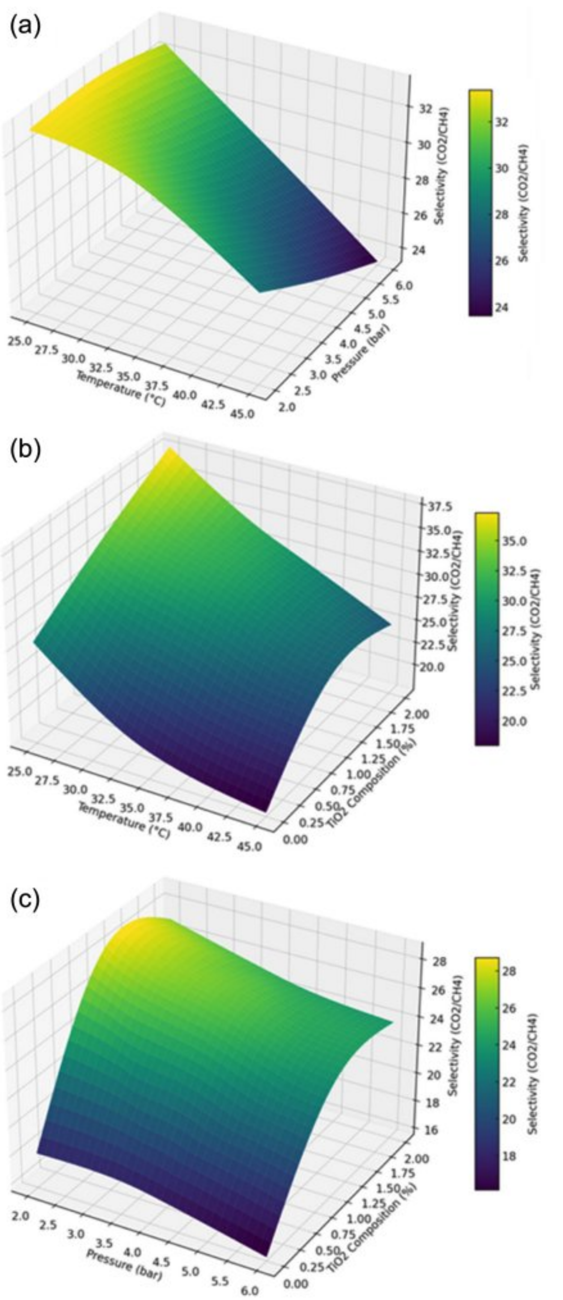

Figure 3. (a) Effect of temperature and pressure on selectivity (CO_2/CH_4) at TiO_2 composition of 1 wt%; (b) effect of temperature and TiO_2 composition on selectivity (CO_2/CH_4) at 4 bar pressure; (c) effect of pressure and TiO_2 composition on selectivity (CO_2/CH_4) at temperature of 45 °C.

The effects of pressure and TiO_2 composition on CO_2 permeance at 35 ℃ are shown in Figure 1(c). At this temperature, dual-sorption characteristics and thermodynamic interactions between the polymer matrix and the permeating gas work together to reduce CO_2 permeance in response to increased feed pressure. The increase in CO_2 permeance with TiO_2 content at 35 ℃ is consistent with findings from Figure 3, showing a maximum permeance of 16.31 GPU at 2 bar and 2 wt% TiO_2, while the minimum permeance is 10.89 GPU at 6 bar for the blend membrane.

CH_4 Permeance. The mathematical representations for CH_4 permeance using real variables and coded components is presented, Equation 5. The empirical model terms and ANOVA findings for CH_4 permeance are shown in Table 4. The results demonstrate that the quadratic model is statistically significant for CH_4 permeance, as evidenced by its F-value of 2.596.

However, the terms including A, B, AB, AC, BC, A^2, and B^2 are found to be insignificant. The temperature appears to have the most impact on CH_4 permeance across the membrane, as indicated by the highest F-value of 14.409 for term C. Furthermore, the divergence between the experimental data and the anticipated CH_4 permeance is confirmed to be within an acceptable range by an R^2 value of 0.579. Nevertheless, the CH_4 model demonstrates lower predictive accuracy compared to the CO_2 model, the overall optimization strategy remains robust. This robustness is largely attributed to the fact that the optimization is primarily governed by separation performance, which is more strongly influenced by the CO_2 permeance model.

$$\begin{aligned} CH_4\ \text{Permeance} &= 0.4644 + 0.0042A + 0.0013B - 0.0683C \\ &+ 0.0001AB - 0.0008AC - 0.0007BC - 0.0003A^2 + 0.000B^2 \\ &+ 0.0406C^2 \end{aligned} \tag{5}$$

The 3D graphs illustrate the effect of TiO_2 temperature, composition, and pressure on the permeance of CH_4 in the PCMs, Figure 2. The behavior of CH_4 permeance in response to increasing temperature and feed pressure is analogous to the CO_2 permeance, Figure 2(a). As temperature decreases, CH_4 permeance rises gradually, reaching a maximum of 0.52 GPU at 25 ℃ and 6 bar. Conversely, an increase in feed pressure diminishes the dual-sorption properties and increases the diffusion properties of CH_4 through the available free volume, leading to a slight rise in CH_4 permeance.

CH_4 permeance decreases modestly with rising temperature due to the reduced solubility of the gas across the membrane surface as temperature increases, Figure 2(b). On the other hand, the addition of TiO_2 has an abrupt decrease in CH_4 permeance of nearly 1 wt% titania, and then a sudden increase is observed as well. This effect is prominent at a temperature of 45 ℃. Furthermore, the increase in feed pressure affects the dual-sorption characteristics and CH_4 solubility coefficient, which leads to a decrease in CH_4 permeance. These results are com-

Table 4. ANOVA Results and Empirical Model Terms of CH_4 Permeance

Sources	Sum of squares	DOF	F-Value	PR(>F)	Mean Square	Significance
A	8.9E-05	1	0.102	0.753	8.9E-05	N-S[b]
B	1.5E-05	1	0.017	0.897	1.5E-05	N-S
C	1.2E-02	1	14.409	0.001	1.2E-02	S[a]
A^2	7.4E-06	1	0.009	0.927	7.4E-06	N-S
B^2	1.9E-06	1	0.002	0.964	1.9E-06	N-S
C^2	9.9E-03	1	11.379	0.004	9.9E-03	S
AB	7.5E-05	1	0.086	0.772	7.5E-05	N-S
AC	3.3E-05	1	0.038	0.847	3.3E-05	N-S
BC	5.3E-04	1	0.615	0.444	5.3E-04	N-S
Residual	1.5E-02	17	-	-	8.7E-04	N-S
R^2	0.579	-	-	-	-	-
Adjusted R^2	0.356	-	-	-	-	-
Model	0.020264	9	2.596	0.043	2.3E-03	S

[a] Significant. [b] Not Significant.

parable to those documented in the literature about CH_4 permeance in ZIF-8/6FDA-durene flat sheet MMMs.[20]

The PCM with a TiO_2 content of 1 wt% at 2 bar had the lowest CH_4 permeance, measuring at 0.47 GPU. By contrast, the highest CH_4 permeance of 0.58 Gas Permeation Units (GPU) is achieved using the smallest amount of TiO_2 and a pressure of 6 bar, Figure 2(c).

CO_2/CH_4 Ideal Selectivity. The details of CO_2/CH_4 selectivity models expressed as coded and real factors, Equation 6. The model's statistical significance is demonstrated by its noteworthy F-value of 42.495. Important terms A, B, BC, A^2, and C^2 in the model for CH_4 permeance. With an R^2 value of 0.957, this model depends on predicting the CO_2/CH_4 separation factor from the three variables involved.

The analysis further highlights the dominant influence of TiO_2 composition, which has the highest F-value of 51.546, indicating a substantial impact on the separation factor. This is followed by temperature and pressure, with F-values of 8.878 and 1.345, respectively, suggesting that while temperature also plays a notable role, the effect of pressure is relatively less sig-

Table 5. ANOVA Results and Empirical Model Terms of CO_2/CH_4 Selectivity

Sources	Sum of squares	DOF	F-Value	PR(>F)	Mean square	Significance
A	3.692	1	1.345	0.262	3.692	N-S[b]
B	24.365	1	8.878	0.008	24.365	N-S
C	141.464	1	51.546	0.000	141.464	S[a]
A^2	0.971	1	0.354	0.560	0.971	N-S
B^2	9.209	1	3.356	0.085	9.209	N-S
C^2	43.072	1	15.694	0.001	43.072	S
AB	1.500	1	0.547	0.470	1.500	N-S
AC	0.106	1	0.039	0.847	0.106	N-S
BC	4.057	1	1.478	0.241	4.057	N-S
Residual	46.655	17	-	-	2.744	N-S
R^2	0.957	-		-	-	-
Adjusted R^2	0.935	-	-	-	-	-
Model	1049.628	9	42.495	0.000	116.625	S

[a] Significant. [b] Not Significant.

nificant in determining the CO_2/CH_4 selectivity, Table 5. The ideal selectivity of the asymmetric membrane is affected by its dense selective layer and other process characteristics that significantly affect its performance.[1,21]

$$\text{Selectivity} = 55.4148 - 0.9194A - 1.2865B + 12.3309C - 0.0177AB - 0.0470AC - 0.0581BC + 0.1006A^2 + 0.0124B^2 - 2.6793C^2 \quad (6)$$

The effect of pressure temperature, and TiO_2 composition on the ideal selectivity is illustrated, Figure 3. The decrease in ideal selectivity with an increase in temperature, likely due to the reduced sorption properties of the more condensable CO_2 gas at higher temperatures, which diminishes its interaction with the membrane surface, leading to a decrease in ideal selectivity, Figure 3(a). The lowest CO_2/CH_4 separation factor observed is 23.39 at 45 ℃ and 6 bar. Furthermore, ideal selectivity also declines with increased feed pressure, correlating with a decrease in CO_2 permeance as pressure rises—a trend consistent with previous studies suggesting reduced gas permeability for polarizable gases like CO_2 under increased pressure in glassy polymers.[22] The maximum separation factor recorded is 33.41 at 4 bar and 25 ℃.

At a constant feed pressure of 4 bar, the effect of temperature and TiO_2 content on the CO_2/CH_4 separation factor is highlighted, Figure 3(b). The separation factor improves as TiO_2 composition rises from 0% to 2% by weight. The optimal selectivity of the PCMs is positively impacted by the addition of TiO_2, as gas flow through the membrane is improved by nanoparticle aggregation and void formation at the TiO_2-polymer interface. The highest ideal selectivity achieved is 41.08 at a TiO_2 composition of 2 wt% and a temperature of 25 ℃. However, an increase in temperature at a TiO_2 composition of 2 wt% results in a decrease in ideal selectivity, with the minimum separation factor of 17.56 at 45 ℃.

The effect of TiO_2 composition and pressure on the optimum selectivity of CO_2/CH_4 at a constant temperature of 35 ℃. At 2 bar of pressure and 1.85 weight percent TiO_2, the maximum optimum selectivity of 32.62 is observed, Figure 3(c).

In contrast, the minimum ideal selectivity of 18.78 is noted at a pressure of 6 bar and in the absence of TiO_2 nanoparticles. These observations underscore the complex interplay of process parameters on membrane performance, particularly how material composition and operating conditions jointly dictate separation efficacy.

Comparison of Predicted and Actual Selectivity. The actual versus predicted selectivity derived from the quadratic model employed in this study showed, Figure 4. The scatter plot points, which represent the actual selectivity values, are plotted against the predicted selectivity values from the model. The proximity of these points to the dashed line, which indicates a perfect correlation between the actual and predicted values, highlights the model's high prediction accuracy.

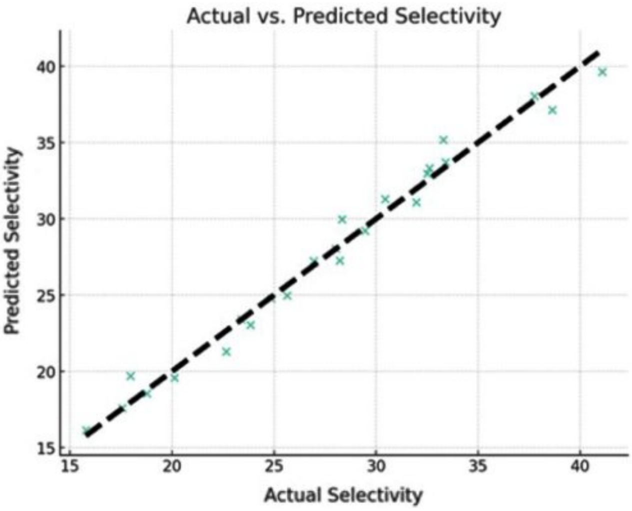

Figure 4. Comparison of actual and predicted selectivity values.

The model's intercept is approximately 29.75, with an R^2 value of 0.9813, indicating a strong fit of the model. The high R^2 score suggests that the model can explain a significant percentage of the variance in selectivity, which is crucial for accurate predictions and optimization. The image shows that the model accurately represents the complex relationship between the influencing variables (pressure, temperature, and TiO_2 composition) and selectivity. This supports the model's robustness and demonstrates its usefulness for optimization and prediction applications.

Conclusions

The study has effectively shown that separating CO_2 and CH_4 can be improved by utilizing membranes made from a blend of PEI-PVAc and TiO_2 nanoparticles. We established optimal conditions that considerably improve the separation performance of these membranes by using a quadratic model and strategically combining RSM and CCD. The experimental results closely match the predicted models, resulting in an R^2 value of 0.9813. This demonstrates a strong correlation and confirms the model's capability to manage the complex connections among process variables.

Adding TiO_2 nanoparticles to the membrane matrix has demonstrated significant advantages in enhancing mechanical stability and separation efficiency. This nanoparticle addition improves the permeability of CO_2 and enhances its selectivity while preserving or reducing the permeability of CH_4 across different operational settings. The study also highlights the critical influence of temperature, pressure, and TiO_2 composition on membrane performance, providing detailed insights into how each factor contributes to overall efficiency.

Acknowledgment: This work was funded by the University of Jeddah, Jeddah, Saudi Arabia, under grant No. (UJ-23-DR-75). Therefore, the authors thank the University of Jeddah for its technical and financial support.

Conflict of Interest: The authors declare that there is no conflict of interest.

References

1. Mubashir, M.; Fong, Y. Y.; Leng, C. T.; Keong, L. K.; Jusoh, N. Study on the Effect of Process Parameters on CO_2/CH_4 Binary Gas Separation Performance Over NH_2-MIL-53(Al)/cellulose Acetate Hollow Fiber Mixed Matrix Membrane. *Polym. Test.* **2020**, 81, 106223.
2. Lai, L. S.; Yeong, Y. F.; Lau, K. K.; Shariff, A. M. Synthesis of Zeolitic Imidazolate Frameworks (ZIF)-8 Membrane and Its Process Optimization Study in Separation of CO_2 From Natural Gas. *J. Chem. Technol. Biotechnol.* **2017**, 92, 420-431.
3. Ding, S. H.; Oh, P. C.; Jamil, A. Effect of Air Gap Interval on Polyvinylidene Fluoride Hollow Fiber Membrane Spinning for CO_2 and CH_4 Gas Separation. *Korean J. Chem. Eng.* **2022**, 39, 2499-2504.
4. Jamil, A.; Ching, O. P.; Iqbal, T.; Rafiq, S.; Zia-ul-Haq, M.; Shahid, M. Z.; Mubashir, M.; Manickam, S.; Show, P. L. Development of An Extended Model for the Permeation of Environmentally Hazardous CO_2 Gas Across Asymmetric Hollow Fiber Composite Membranes. *J. Hazard. Mater.* **2021**, 417, 126000.
5. Yuan, H.; Liu, J.; Zhang, X.; Chen, L.; Zhang, Q.; Ma, L. Recent Advances in Membrane-based Materials for Desalination and Gas Separation. *J. Cleaner Prod.* **2023**, 387, 135845.
6. Chen, X. Y.; Vinh-Thang, H.; Ramirez, A. A.; Rodrigue, D.; Kaliaguine, S. Membrane Gas Separation Technologies for Biogas Upgrading. *RSC Adv.* **2015**, 5, 24399-24448.
7. Jamil, A.; Ching, O. P.; Shariff, A. M. Polymer-Nanoclay Mixed Matrix Membranes for CO_2/CH_4 Separation: A Review. *Appl. Mechanics Mater.* **2014**, 625, 690-695.
8. Wong, K. K.; Jawad, Z. A. A Review and Future Prospect of Polymer Blend Mixed Matrix Membrane for CO_2 Separation. *J. Polym. Res.* **2019**, 26, 289.
9. Farrukh, S.; Javed, S.; Hussain, A.; Mujahid, M. Blending of TiO_2 Nanoparticles with Cellulose Acetate Polymer: to Study the Effect on Morphology and Gas Permeation of Blended Membranes. *Asia-Pac. J. Chem. Eng.* **2014**, 9, 543-551.
10. Li, J.-F.; Xu, Z.-L.; Yang, H.; Yu, L.-Y.; Liu, M. Effect of TiO_2 Nanoparticles on the Surface Morphology and Performance of Microporous PES Membrane. *Appl. Surf. Sci.* **2009**, 255, 4725-4732.
11. Madaeni, S. S.; Badieh, M. M. S.; Vatanpour, V.; Ghaemi, N. Effect of Titanium Dioxide Nanoparticles on Polydimethylsiloxane/polyethersulfone Composite Membranes for Gas Separation. *Polym. Eng. Sci.* **2012**, 52, 2664-2674.
12. Ahmad, J.; Deshmukh, K.; Hägg, M. B. Influence of TiO_2 on the Chemical, Mechanical, and Gas Separation Properties of Polyvinyl Alcohol-Titanium Dioxide (PVA-TiO_2) Nanocomposite Membranes. *Int. J. Polym. Anal. Charact.* **2013**, 18, 287-296.
13. Hu, Q.; Marand, E.; Dhingra, S.; Fritsch, D.; Wen, J.; Wilkes, G. Poly(amide-imide)/TiO_2 Nano-composite Gas Separation Membranes: Fabrication and Characterization. *J. Membr. Sci.* **1997**, 135, 65-79.
14. Maqsood, K.; Jamil, A.; Ahmed, A.; Sutisna, B.; Nunes, S.; Ulbricht, M. Effect of TiO_2 on Thermal, Mechanical, and Gas Separation Performances of Polyetherimide-Ndash; Polyvinyl Acetate Blend Membranes. *Membranes* **2023**, 13, 734.
15. Maqsood, K.; Jamil, A.; Ahmed, A.; Sutisna, B.; Nunes, S.; Ulbricht, M. Blend Membranes Comprising Polyetherimide and Polyvinyl Acetate with Improved Methane Enrichment Performance. *Chemosphere* **2023**, 321, 138074.
16. Zhuang, G.-L.; Tseng, H.-H.; Uchytil, P.; Wey, M.-Y. Enhancing the CO_2 Plasticization Resistance of PS Mixed-matrix Membrane by Blunt Zeolitic Imidazolate Framework. *J. CO_2 Util.* **2018**, 25, 79-88.
17. Muruganandam, N.; Paul, D. R. Gas Sorption and Transport in Miscible Blends of Tetramethyl Bisphenol-A Polycarbonate and Polystyrene. *J. Polym. Sci., Part B: Polym. Phys.* **1987**, 25, 2315-2329.
18. Li, Y.; Chen, D.; He, X. Preparation and Characterization of Polyvinylalcohol/Polysulfone Composite Membranes for Enhanced CO_2/N_2 Separation. *Polymers* **2023**, 15, 124.
19. Azizi, N.; Mohammadi, T.; Behbahani, R. M. Synthesis of a New Nanocomposite Membrane (PEBAX-1074/PEG-400/TiO_2) in Order to Separate CO_2 from CH_4. *J. Nat. Gas Sci. Eng.* **2017**, 37, 39-51.
20. Jusoh, N.; Yeong, Y. F.; Lau, K. K.; Shariff, A. M. Transport Properties of Mixed Matrix Membranes Encompassing Zeolitic Imidazolate Framework 8 (ZIF-8) Nanofiller and 6FDA-durene Polymer: Optimization of Process Variables for the Separation of CO_2 from CH_4. *J. Cleaner Prod.* **2017**, 149, 80-95.
21. Ismail, A. F.; David, L. I. B. A Review on the Latest Development of Carbon Membranes for Gas Separation. *J. Membr. Sci.* **2001**, 193, 1-18.
22. Sanaeepur, H.; Amooghin, A. E.; Moghadassi, A.; Kargari, A. Preparation and Characterization of Acrylonitrile–butadiene–styrene/poly(vinyl acetate) Membrane for CO_2 Removal. *Sep. Purif. Technol.* **2011**, 80, 499-508.